IAEA-ICTP Workshop 2019
Atomic and Molecular Spectroscopy in Plasmas
Lecture: Spectral Line Broadening

S. Ferri

Aix-Marseille University, CNRS, PIIM, France

sandrine.ferri@univ-amu.fr

May 7, 2019

Emitted radiation from plasmas

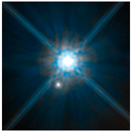

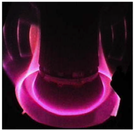

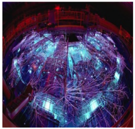

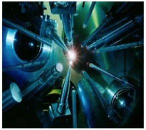

The emitted radiation is usually the only observable quantity to obtain information on plasmas.

Information contained in a spectrum

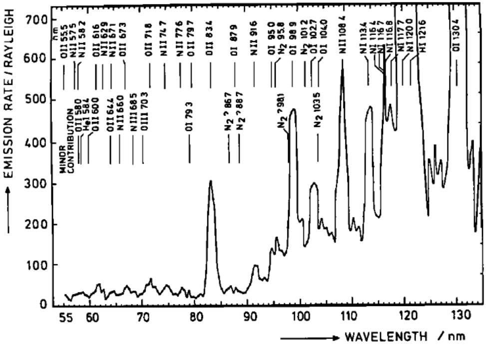

Fig. 1a: Auroral EUV Emission Spectrum (Sum of 8 Scans)

[1]

The information contained in a spectrum is related to both:

- the atomic physics of chemical elements in the medium
- the plasma physics of the environment

[1] Fischer et al., Geophys. Res. Lett., 7: 1003 (1980)

Origins of the radiation

The radiation field in a plasma can originate from three types of radiative transitions:

- **bound-bound transitions**: present a peak intensity at a frequency corresponding to the energy difference between two bound levels.
- **bound-free transitions**: recombination radiation
- **free-free transitions**: Bremsstrahlung radiation

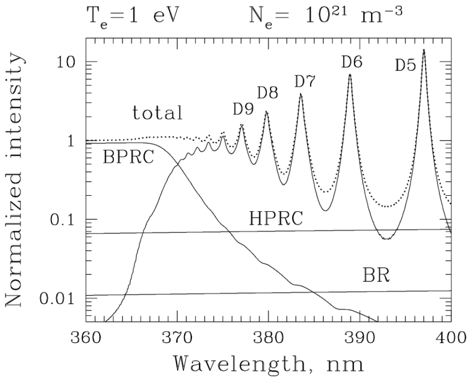

Figure 2. Basic components of the emission spectrum from a pure deuterium p explanations in the text).

2

[2] A.Y. Pigarov et al., PPCF40 ,2055 (1998).

Line intensity distribution

The line intensity distribution is given by:

$$I_\omega = N_u A_{u\ell} \hbar\omega_{u\ell} L(\omega) \qquad (1)$$

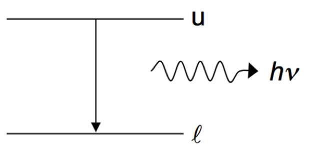

where

- N_u is the upper level population density,
- $A_{u\ell}$ is the rate of spontaneous radiative decay,
- $h\nu_{u\ell} = \hbar\omega_{u\ell} = E_u - E_\ell$ is the emitted photon energy,
- $L(\omega)$ is the **line profile**.

Line profiles

Normalized line profile:

$$\int L(\omega)d(\omega) = 1 \qquad (2)$$

or

$$\int L(\lambda)d(\lambda) = 1 \qquad (3)$$

with

$$L(\lambda) = \frac{2\pi c}{\lambda^2} L(\omega) \qquad (4)$$

Full Width at Half Maximum (FWHM): $\Delta\lambda_{1/2}$.

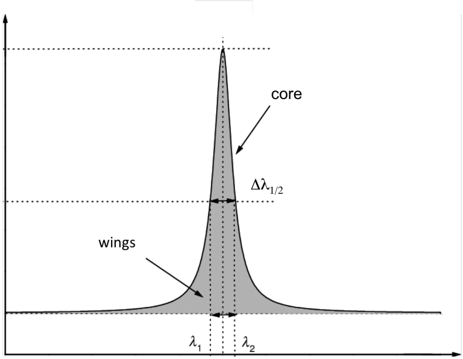

A line in a spectrum is most completely characterized by its profile → **connection to the intrinsic properties of the medium**

Lines shapes in plasmas are important since

- they are needed for a detailed model/calculation of line intensity distribution,
- line broadening can be sensitive to the:
  - temperature (Doppler broadening)
  - density (Stark broadening)
  - magnetic field (Zeeman splitting)

  → spectroscopic diagnostics
- needed for modeling the radiation transport.

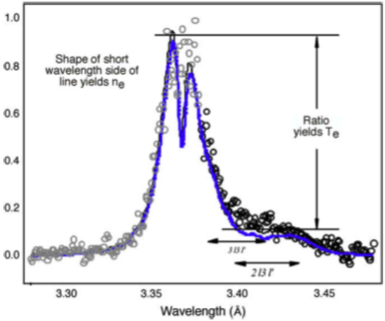

Ar He$-\beta$ line and its satellites: diagnostics of N_e and T_e on single spectrum

[3],[4]

[3]N.C. Woolsey et al., Phys. Rev. E **53**, 6396 (1996)

[4]H.K. Chung and R.W. Lee, International J. of Spec., 506346 (2010)

A suite of codes for modeling spectra

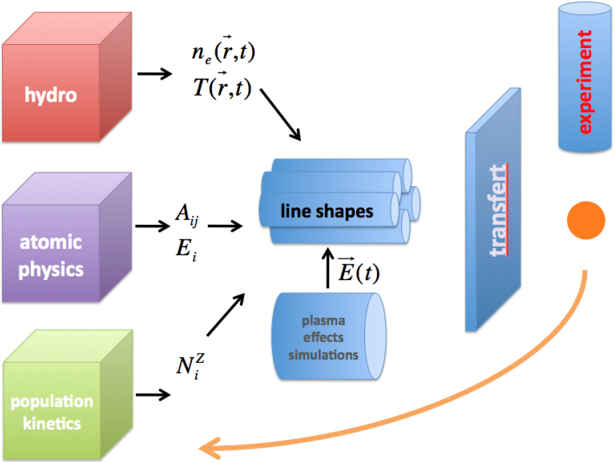

Line shape modeling in plasmas has a long history

- in the 60's: theory of spectral line broadening in plasmas is born[1,2]
- in the 70's: the observed deviations between experiments and theories were attributed to ion motion → first attempts to include ion motion effects on theories [3-6]. Experimental proof on hydrogen is obtained [7].
- from the 80's: first N-body simulations [8-12] and sophisticated models for neutral emitters or multicharged emitters of various complexity and applicability [13-19]

[1] M. Baranger, Phys. Rev. **111**, 481 (1958); Phys. Rev. **111**, 494 (1958); Phys. Rev. **112**, 855 (1958)

[2] A.C. Kolb and H.R. Griem, Phys. Rev. **111**, 514 (1958)

[3] J. Dufty, Phys. Rev. A **2** (1970)

[4] U. Frish and A. Brissaud, J.Q.S.R.T. **11** (1972)

[5] J.D. Hey, H.R. Griem, Phys. Rev. A **12** (1975)

[6] A.V. Demura et al., Sov. Phys. JETP **46** (1977)

[7] D.E. Kelleher, W.L. Wiese, Phys. Rev. Lett. **31** (1973)

[8] R. Stamm and D. Voslamber, J.Q.S.R.T. **22** (1979)

[9] J. Seidel, Spectral Line Shape conf. proc **4** (1987)

[10] G.C. Hegerfeldt, V. Kesting, Phys. Rev. A **37** (1988)

[11] V. Cardenoso, M.A. Gigosos, Phys. Rev. A **39** (1989)

[12] E. Stambulchik and Y. Maron, J. Quant. Spectr. Rad. Transfer 99, 730749 (2006)

[13] C. Fleurier, JQSRT, 17, 595 (1977)

[14] D.B. Boercker, C.A. Iglesias and J.W. Dufty, Phys. Rev. A **36** (1987)

[15] R. C. Mancini, et al., Jr. Computer Physics Communications v63, p314 (1991)

[16] B. Talin, A. Calisti et al., Phys. Rev. A **51** (1995)

[17] S. Lorenzen, et al., Contrib. Plasma Phys. **48** (2008)

[18] B. Duan, et al., Phys. Rev. A **86** (2012)

[19] S. Alexiou, High Energy Density Physics 9, 375(2013)

Overview

1. Introduction
2. Broadening and fluctuations
3. Line broadening in plasmas
   - Natural broadening
   - Doppler broadening
   - Stark broadening
4. Conclusion

Broadening and fluctuations[5]

- For any atomic system embedded in a medium, the interactions between the atomic system and the medium result in a modification of the energies and lifetimes of the atomic system.
- Broadening is in general associated with **fluctuations** and **randomness** is **essential**
- **fluctuations**, i.e. different atoms in a plasma see a different interaction.
- **randomness** is a requirement for broadening.

[5] S. Alexiou, High Energy Density Physics 5, 225 (2009).

- Single velocity:

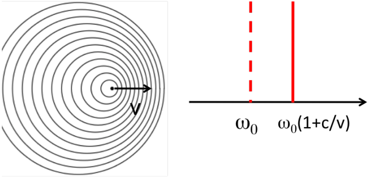

→ **Doppler shift**

- Distribution of velocities:

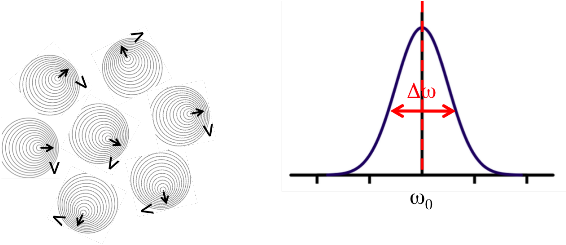

→ **Doppler broadening**

Second example: Exciting a tuning fork[6]

A simple, low-cost, intuitive model for natural and collisional line broadening mechanisms.

- No collision:

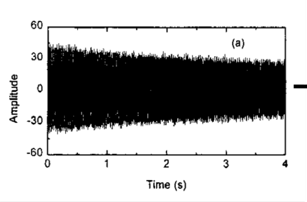

FT $\rightarrow$

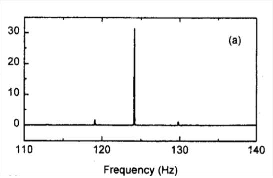

$\rightarrow$ **Delta function**

- Random collisions:

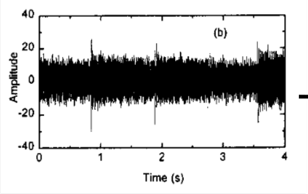

FT $\rightarrow$

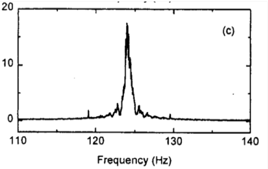

$\rightarrow$ **Broadened shape**

[6] A. Boreen et al., Am. J. Phys. 68, 8 (2000)

Simple case of spectral broadening (I)

- Consider an atomic oscillator of amplitude $A(t)$ emitting a radiation without interruptions:

$$A(t) = A_0 e^{i\omega_0 t} \tag{5}$$

- The Fourier Transform of the amplitude is,

$$\tilde{A}(\omega) = \frac{1}{\sqrt{2\pi}} \int_{-\infty}^{+\infty} A(t) e^{-i\omega t} dt = A_0 \delta(\omega - \omega_0) \tag{6}$$

- The Fourier spectrum is monochromatic and characterized by a delta function.
- The energy spectrum, defined as $E(\omega) = \frac{1}{2\pi} A(\omega) A^*(\omega)$, is a direct measure of the energy in the wave train at frequency ω.

Simple case of spectral broadening (II)

- The spectral line is related to the energy delivered per time unit, i.e. the power spectrum given by

$$I(\omega) = \lim_{T\to\infty} \frac{1}{2\pi T} \left| \int_{-T/2}^{+T/2} A(t) e^{-i\omega t} dt \right|^2 \tag{7}$$

- or in term of correlation function

$$I(\omega) = \int_{-\infty}^{+\infty} C(t) e^{-i\omega t} dt \tag{8}$$

- Thus, the power spectrum is characterized by a delta function

$$I(\omega) = \frac{A_0^2}{\pi} \delta(\omega - \omega_0) \tag{9}$$

Simple case of spectral broadening (II)

- Consider that the emitted radiation is interrupted due to an interaction with another particle in the plasma, so that is occurs only for a finite time interval from $-t_0$ to $+t_0$, the Fourier Transform becomes,

$$\tilde{A}(\omega) = \frac{1}{\sqrt{2\pi}} \int_{-t_0}^{+t_0} A(t) e^{-i\omega t} dt = A_0 \sqrt{\frac{2}{\pi}} \frac{sin(\omega - \omega_0) t_0}{(\omega - \omega_0)} \tag{10}$$

- The emission is no longer monochromatic and there is an effective broadening of the spectrum.
- The more frequent the interactions, the sorter t_0 and the broader the profile.

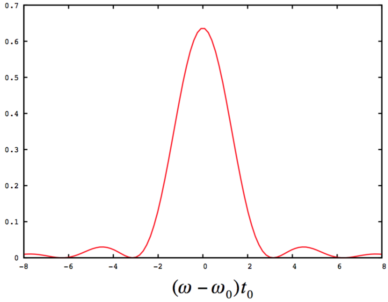

No more simple case of spectral broadening (III)

Assuming, now, that we observe an ensemble of atomic oscillators interacting with other particles in the plasma.

The power spectrum results is finite with a frequency distribution proportional to the energy spectrum of an individual oscillator.

The interaction term can be decomposed into a mean term plus a fluctuating one:

$$V(t) = < V > + \delta v(t) \tag{11}$$

- mean term $< V > \rightarrow$ set of infinitively sharp energies.

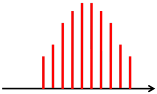

$\rightarrow$ inhomogeneous broadening

- fluctuating term $\delta v(t)$ is a measure of disorder.

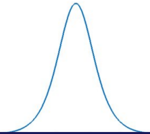

$\rightarrow$ homogeneous broadening

Overview

Natural broadening (I)

- Results from the finite life time of the upper (u) and lower levels (l)

- Heisenberg 's uncertainty principle:

$$\Delta E \Delta t \geqslant \hbar/2 \textit{ with } \Delta t \approx \frac{1}{\Gamma} \qquad (12)$$

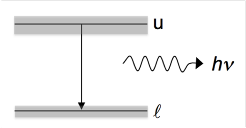

where Γ includes all atomic decay rates: $\Gamma = \sum A_{u\ell}$

- The amplitude has a damped oscillatory time dependence:

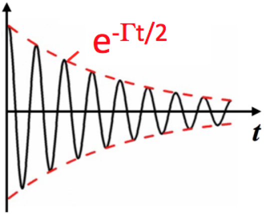

$$A(t) = A_0 e^{i\omega_0 t} e^{-\frac{\Gamma}{2}t} \qquad (13)$$

$$\downarrow \text{FT}$$

$$\tilde{A}(\omega) = -\frac{A_0}{\sqrt{2\pi}} \frac{1}{\left(\Gamma/2 + i(\omega - \omega_0)\right)} \qquad (14)$$

Natural broadening (II)

- And, from the power spectrum we can extract a Lorenztian line shape function:

$$L_N(\omega) = \frac{1}{\pi} \frac{\Gamma/2}{\left((\omega - \omega_0)^2 + (\Gamma/2)^2\right)}, \tag{15}$$

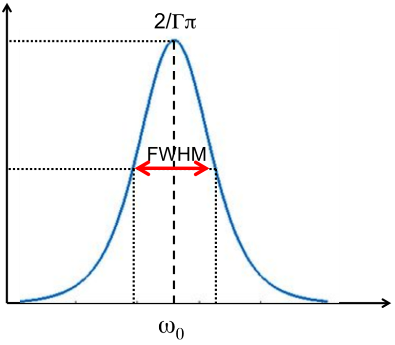

- which is normalized:

$$\int_{-\infty}^{+\infty} L_N(\omega) d\omega = 1 \tag{16}$$

- Full Width at Half Width at Maximum (FWHM):

$$FWHM = \Gamma \tag{17}$$

Natural broadening (III)

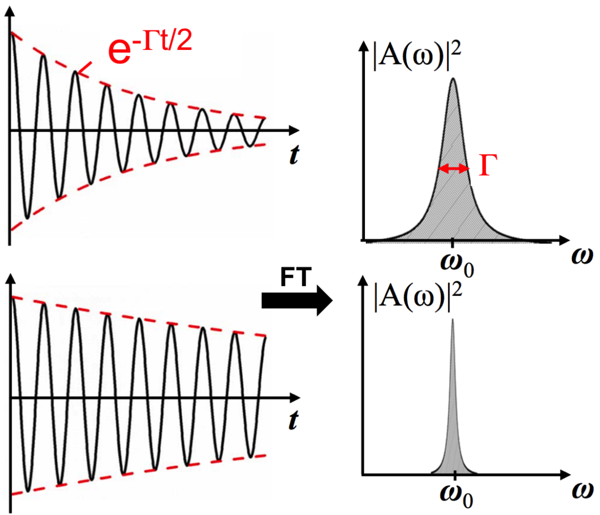

Natural broadening (IV)

Independent of the environment of the radiating atom.

Typical values:

- Electronic transitions:
  $\Gamma \sim 10^8 s^{-1} \quad \rightarrow \quad FWHM \sim 10^{-7} eV$
- Vibrational-rotational transitions:
  $\Gamma \sim 10^2 s^{-1} \quad \rightarrow \quad FWHM \sim 10^{-13} eV = 10^{-10} cm^{-1}$

Generally, negligible compared to Doppler and plasma broadening.

Doppler broadening (I)

Results from the thermal/microscopic motion of the radiators (ions) in a plasma.

The Doppler effect tells us that the frequency of radiation depends on the motion of source and observer. Doppler-shifted frequency for a radiator moving at velocity v along the line of sight differs from ω_0 in rest frame of atom.

- in rest frame of the radiator:

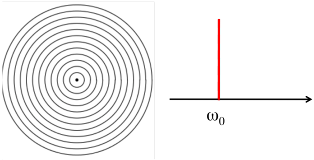

- in rest frame of the observer:

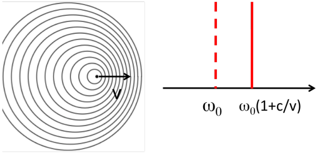

Doppler broadening (II)

- The amplitude of the radiation emitted by a fixed radiator at position $\vec{r}$, at time t:

$$A(\vec{r}, t) \propto e^{i(\omega_0 t - \vec{k}_0 \cdot \vec{r})} \tag{18}$$

with $\vec{k}_0$ the wave number vector and ω_0 the oscillation frequency.

- for a moving radiator:

$$A(\vec{r}, t) \propto e^{i(\omega_0 t - \vec{k}_0 \cdot \vec{r}(t))} \text{ with } \vec{r}(t) = \vec{r}_0(t) + \int_0^t \vec{v}(t')dt' \tag{19}$$

- Now if we consider an ensemble of moving radiators that never collide nor never change their velocities, we have to determine the autocorrelation function:

$$C(t) = Re\langle e^{i(\omega_0 \tau - \vec{k}_0 \cdot \vec{r}(\tau))} \rangle \text{ where } \vec{r}(\tau) = \int_t^{t+\tau} \vec{v}(t')dt' = \vec{v}\tau \tag{20}$$

Doppler broadening (III)

- for a Maxwellian velocity distribution within the ensemble,

$$f(\vec{v}) = \left(\frac{M_i}{2\pi k_B T_i}\right)^{3/2} e^{-\frac{M_i |\vec{v}|^2}{2\pi k_B T_i}} \qquad (21)$$

- the Fourier Transform then yields the area normalized Doppler lin profile.

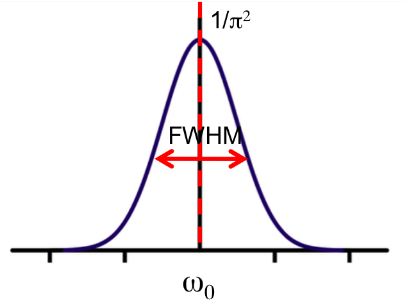

- The corresponding normalized line shape function is Gaussian,

$$L_D(\omega) = \frac{1}{\sqrt{\pi}\omega_D} e^{-(\Delta\omega/\omega_D)^2}, \qquad (22)$$

- with $\Delta\omega = \omega - \omega_0$
- and ω_D, the Doppler broadening parameter given by,

$$\omega_D = \sqrt{\frac{2k_B T_i}{M_i c^2}}\omega_0 \qquad (23)$$

Doppler broadening (II)

$$FWHM = 2\sqrt{ln2}\omega_D = \omega_0 \cdot 7.715 \times 10^{-5}\sqrt{\frac{T_i(eV)}{M_i(u)}} \tag{24}$$

Dominant for H, D, T and He in Tokamak plasmas.

It is of the order of 1 eV in hot plasmas, i.e. for temperatures of the order of 1 keV

Voigt line shape

The combined effect of natural and Doppler broadening is given by convolution of the Lorenztian and Gaussian functions.

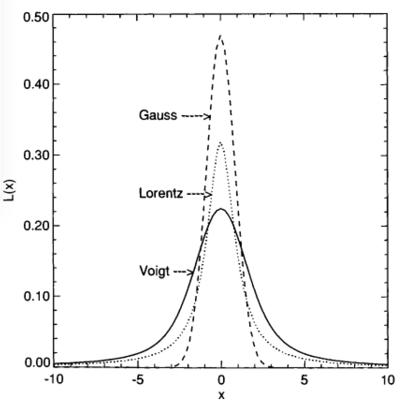

©Griem, Principle of Plasma Spectroscopy, (1997)

This is the Voigt line shape:

$$L_v(\omega) = H(a, V) = \frac{a}{\pi} \int_{-\infty}^{+\infty} \frac{e^{-y^2} dy}{(v-y)^2 + a^2} \quad (25)$$

with

$$V = \frac{\omega - \omega_0}{\Delta\omega_D} \qquad a = \frac{\Gamma}{4\pi\Delta\omega_D}$$

(26)

Stark effect (I) - Basics

The Stark effect is the shifting and splitting of spectral lines of atoms and molecules due to the presence of electric fields.

Unperturbed system

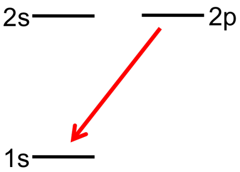

Coupling the dipole with an electric field

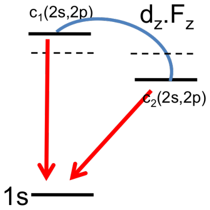

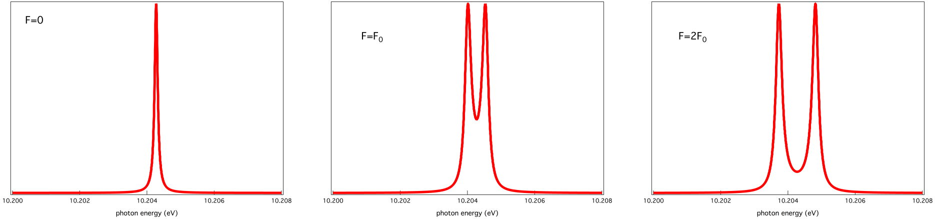

Stark effect (II) - linear vs quadratic Stark effect

Accounting for fine structure

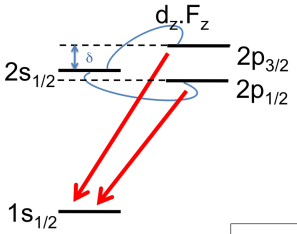

- If $\vec{d} \cdot \vec{F} \ll \delta$
  $\rightarrow$ quadratic Stark effect, e.g. Stark shift $\sim (dF)^2$,
- If $\vec{d} \cdot \vec{F} \gg \delta$
  $\rightarrow$ linear Stark effect, e.g. Stark shift $\sim (dF)$.

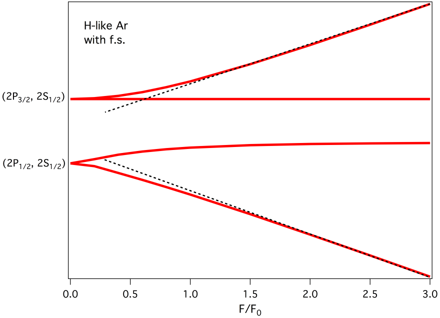

Stark effect (III) - linear vs quadratic Stark effect

Accounting for fine structure

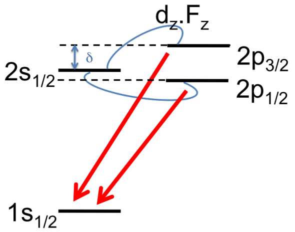

- If $\vec{d} \cdot \vec{F} \ll \delta$
  $\rightarrow$ quadratic Stark effect, e.g. Stark shift $\sim (dF)^2$,

- If $\vec{d} \cdot \vec{F} \gg \delta$
  $\rightarrow$ linear Stark effect, e.g. Stark shift $\sim (dF)$.

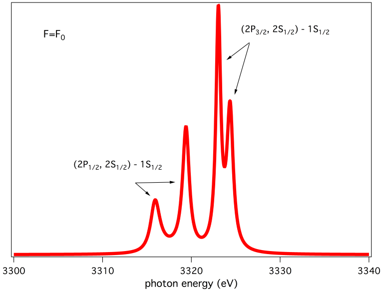

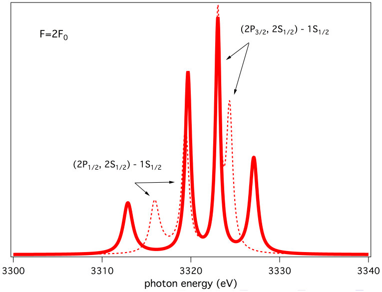

Stark effect (IV) - as a diagnostic tool

- What is the simple link between the electron density N_e and the Stark effect?

- For the case of linear Stark effect, the frequency shift $\Delta\omega \propto (dF)$.

Stark effect (IV) - as a diagnostic tool

- What is the simple link between the electron density N_e and the Stark effect?

- For the case of linear Stark effect, the frequency shift $\Delta\omega \propto (dF)$.
- Considering the normal field strength

$$F_0 = (e/r_0^2) \quad \text{with} \quad r_0 = (\frac{3}{4\pi N_e})^{1/3} \tag{27}$$

where r_0 is the mean interparticle distance.

- The frequency shift is then

$$\Delta\omega \propto N_e^{2/3} \tag{28}$$

Stark broadening in plasmas

The radiators in plasmas are embedded in a bath of moving charged particles that create electric microfields.

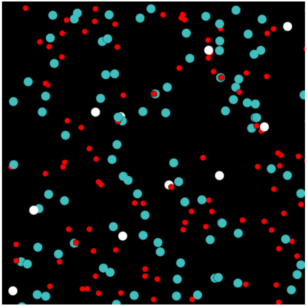

MD simulation of protons, electrons and H emitters

- One of the difficulties is to properly characterize the environment of the emitter.

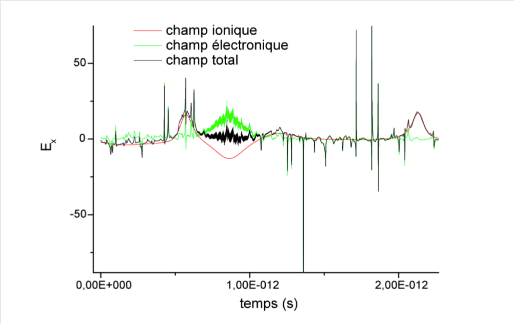

Modeling Stark broadening of lines in plasmas is a complex problem due to the stochastic behavior of the electric microfields $\rightarrow \vec{d} \cdot \vec{F}(t)$

Formalism (I)

- The line shape is given by

$$L(\omega) = \frac{1}{\pi}\int_0^\infty e^{i\omega t} C(t)\, dt, \tag{29}$$

where $C(t)$ is the autocorrelation function of the light amplitude.

- In the dipole approximation and neglecting stimulated emission,

$$C(t) = \sum_{if} e^{-i\omega_{if} t} |\langle f|\vec{d}|i\rangle|^2 \rho \quad \equiv \quad Tr[\vec{d}T^\dagger(t)\vec{d}T(t)\rho], \tag{30}$$

- Here,
  - the trace Tr is the sum over all the states contributing to the line,
  - $\vec{d}$ is the dipole momentum of the radiator,
  - $T(t) = e^{-iHt/\hbar}$ is the evolution operator,
  - H the Hamiltonian of the entire system $H = H_r + H_p + V_{rp}$
  - ρ is the statistical or density operator,

Formalism (II)

Assumptions and approximations:

- density operator of the radiator ρ_r and that of perturbers ρ_p are assumed independent
- the plasma particles perturb the radiator but not the reverse
- the plasma perturbers are classical

$\rightarrow$ statistical average over the perturbers states and quantum treatment over the radiators states:

$$C(t) = Tr_r[\{\vec{d}T_r^\dagger(t)\vec{d}T_r(t)\}_{moy}\rho_r] \tag{31}$$

Using the Liouville operator representation[7]:

$$C(t) = Tr_r[\vec{d}\langle U_l(t)\rangle\vec{d}\rho_r] \tag{32}$$

where $\langle\cdots\rangle$ replaces $\{\cdots\}_{moy}$
and $U_l = e^{-iL_lt}$ is the evolution operator for a given configuration of the system.

[7] U. Fano, Phys. Rev. 131, 259 (1963)

Formalism (III)

The problem is reduced into:

a) finding time evolution of $U_I = e^{-iL_I t}$ accounting for the plasma particles (ions and electrons) perturbation

$$L_I(t) = L_0 - \frac{1}{\hbar}\vec{d} \cdot \vec{F}_I(t) \tag{33}$$

b) averaging its autocorrelation function over a statistically representative ensemble of plasma particles.

$\rightarrow$ cannot be solved analytically due to the stochastic behavior of the perturbation

Method 1) Numerical simulations

Method 2) Models

Formalism (III)

The problem is reduced into:

a) finding time evolution of $U_l = e^{-iL_l t}$ accounting for the plasma particles (ions and electrons) perturbation

$$L_l(t) = L_0 - \frac{1}{\hbar}\vec{d} \cdot \vec{F}_l(t) \tag{34}$$

b) averaging its autocorrelation function over a statistically representative ensemble of plasma particles.

$\rightarrow$ cannot be solved analytically due to the stochastic behavior of the perturbation

Method 1) **Numerical simulations**

Method 2) Models

Numerical Simulations(I) [8],[9],[10],[11],[12]

Numerical integration of the Schrödinger equation in 3 steps

1. Generation of the microfields histories

- N-body plasma simulations
  → particles trajectories
- Electric microfields measurement at the radiators

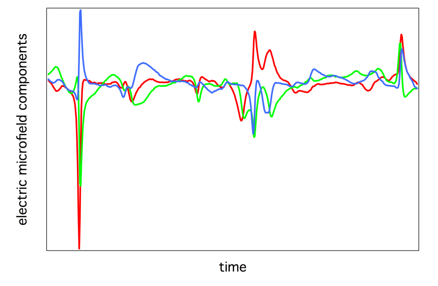

[8] R. Stamm and D. Voslamber, JQSRT **22**, 599 (1979)
[9] W. Olchawa, JQSRT 74, 417 (2002)
[10] M. Gigosos and M. González, JQSRT, 105, 533 (2007).
[11] E. Stambulchik and Y. Maron, HEDP **6**, 9 (2010)
[12] J. Rosato et al., PRE, 79, 046408 (2009).

2. Numerical resolution of the equation of evolution

$$\begin{cases} \frac{dU_l(t)}{dt} = -i\left(L_0 - \frac{1}{\hbar}\vec{d}\cdot\vec{F}_l(t)\right)U_l(t) \\ U_l(0) = \mathbf{1}. \end{cases} \tag{35}$$

$$\downarrow$$

$$U_l(t) \text{ and } C_l(t)$$

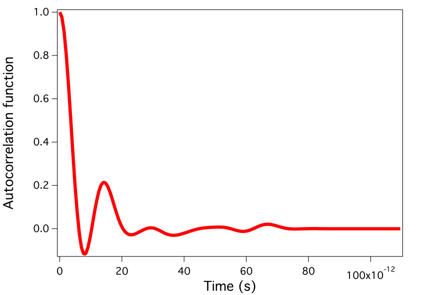

Numerical Simulations (III)

3. Line shape calculations

- Fourier Transform
- Averaging

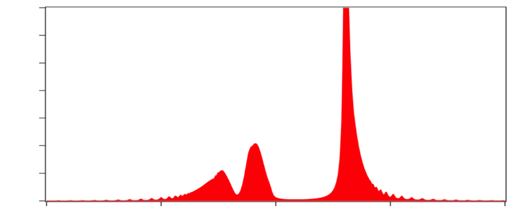

Numerical Simulations (IV)

☺ accounting for the microfields fluctuations

☺ test bed for models

☹ suitable for not too large atomic systems

☹ computer cost

☹ cannot be easily implemented in other codes

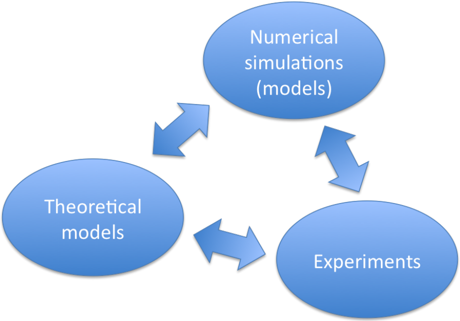

Frequency Fluctuations Model (FFM) compared to Molecular Dynamics simulations[13]

ICF implosion core plasmas applications:

Argon Lyman$-\alpha$ lines for $T_e = 1\ keV$ and $N_e = 1.5 \times 10^{23}\ cm^{-3}$

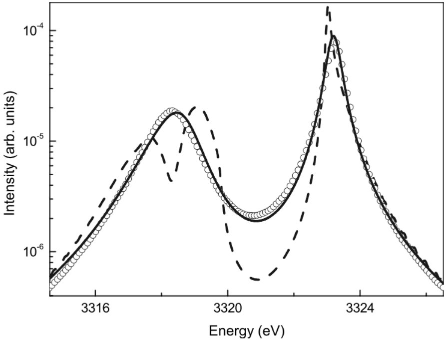

FIG. 1. Lyman-α line with fine structure at $N_e = 1.5 \times 10^{23}$ cm^{-3} and $T_e = 10^7$ K. Comparisons between static profile (dash line), dynamic profile (full line) and molecular dynamics simulation calculation (circles).

[13] A.Calisti et al., Phys. Rev. E 81, 016406 (2010)

Numerical Simulations (VI)

BID (C. Iglesias et al.) and FFM (A. Calisti et al.) compared to SimU line shape simulations (E. Stambulchik et al.)[14].

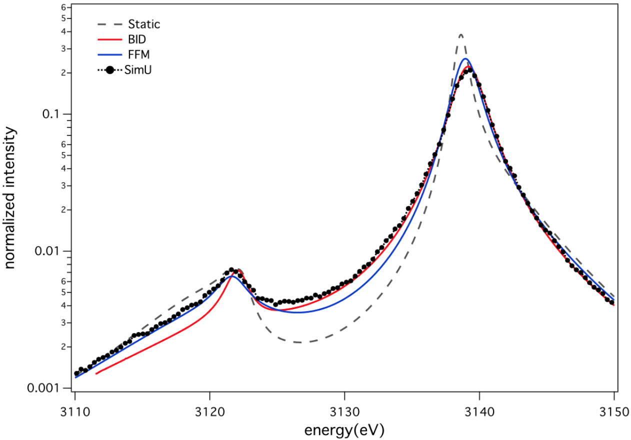

Argon He$-\beta$ lines for $T_e = 1\ keV$ and $N_e = 2 \times 10^{24}\ cm^{-3}$

[14] S. Ferri et al., Atoms 2, 299 (2014)

For the investigation on plasma effects, different plasma models can be simulated[15]

- Interacting ions + electrons simulations: FMD
- Independent ions+ electrons simulations: TMD
- Interacting ions + electrons simulations: FMD-ions
- Interacting electrons + electrons simulations: FMD-electrons
- Independent ions simulations: TMD-ions
- Independent electrons simulations: TMD-electons

H-α lines

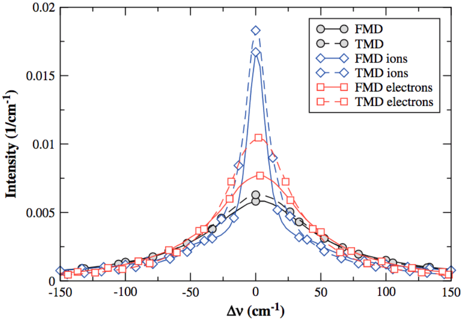

Fig. 1. Comparison of the FMD and TMD results. The contributions of ions and electrons are given separately. The line shapes are area-normalized. Here and in the other figures, $N_e = 10^{18}$ cm^{-3} and $T_e = T_i = 1$ eV are assumed.

[15] E. Stambulchik et al., HEDP 3, 272 (2007).

Formalism (III)

The problem is reduced into:

a) finding time evolution of $U_I = e^{-iL_I t}$ accounting for the plasma particles (ions and electrons) perturbation

$$L_I(t) = L_0 - \frac{1}{\hbar}\vec{d} \cdot \vec{F}_I(t) \tag{36}$$

b) averaging its autocorrelation function over a statistically representative ensemble of plasma particles.

$\rightarrow$ cannot be solved analytically due to the stochastic behavior of the perturbation

Method 1) simulations

Method 2) **Models**

A question of point of view[16]...

time of interest $\tau_i \sim 1/\Delta\omega_{1/2}$ vs inverse of field fluctuation rate $\nu_F \sim v_{th}/r_0$

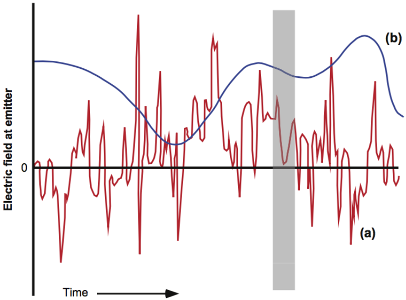

Fig. 4. Different temporal behavior of $V(t)$ over the T time scale. We may have a spiky field (a), a smooth field (b) or even an essentially constant field (b, if the time scale is the shaded area).

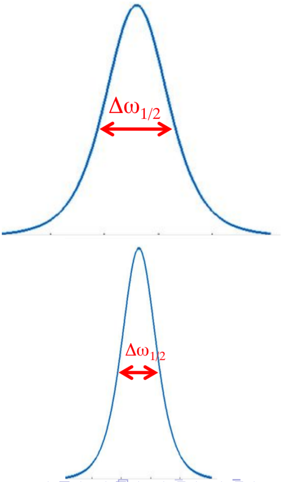

[16] S. Alexiou, HEDP 5, 225 (2009)

Models (I) - Point of view

A question of point of view[17]...

time of interest $\tau_i \sim 1/\Delta\omega_{1/2}$ vs inverse of field fluctuation rate $\nu_F \sim v_{th}/r_0$

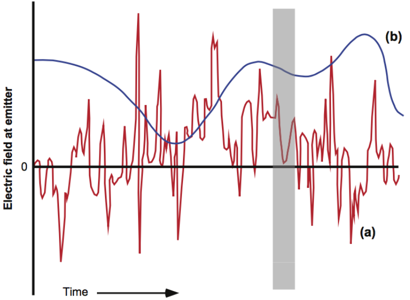

Fig. 4. Different temporal behavior of $V(t)$ over the T time scale. We may have a spiky field (a), a smooth field (b) or even an essentially constant field (b, if the time scale is the shaded area).

- If $\tau_i \gg \nu_F$ then **collisional models** can be used
- If $\tau_i \ll \nu_F$ then **quasi-static approximation** can be used
- $\rightarrow$ Are the high-n lines more or less static than low-n lines?

[17] S. Alexiou, HEDP 5, 225 (2009)

Standard Theory (I)

Standard Theory: the effects of the plasma environment on the radiator are splitted into two parts characterized by two radically different frequency regions.

$$\frac{\nu_e}{\nu_i} \sim \sqrt{\frac{m_e}{M_i}} Z_i^{1/3} \tag{37}$$

e.g. for protons: $\frac{\nu_e}{\nu_i} \sim 40$ for Argon: $\frac{\nu_e}{\nu_i} \sim 250$

$\rightarrow$ the slow ions and fast electrons: $\langle \cdots \rangle = \langle \langle \cdots \rangle_{electrons} \rangle_{ions}$

The two extreme approximations:

- **impact approximation** for the electrons $\rightarrow$ collisional operator is used:

$$\langle \cdots \rangle_{electrons} \rightarrow \frac{1}{\omega - L(F_i) - i\phi_e} \tag{38}$$

- **static approximation** for the ions $\rightarrow$ static microfields are considered:

$$\langle \cdots \rangle_{ions} \rightarrow \int_0^\infty dF_i W(F_i)(\cdots) \tag{39}$$

Impact approximation (I)

Memory loss is produced incrementally each collision contributes its share, which is normally small.

Essentially this approximation works by taking advantage of the fact that e-collisions are either weak or dominated by a single strong collision, which means there is no many-body problem.

→ **Strong collision model**:They are isolated in time. They completely interrupt the train wave.

→ **Weak collision model**: Individual collisions are not able to break the coherence. The lost of correlation is due to cumulative effect.

Impact approximation (II) - Strong collisions

Weisskopf theory:

- Plasma free electrons move along straight line trajectories with contant velocity.
- Binary collision involving the radiator and one free electron.
- Duration of the collision is much shorter that the atomic state's lifetime.
- Collisions are elastic and does not induce transitions among energy levels.

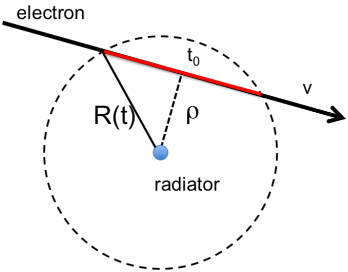

$$R(t) = \sqrt{\rho^2 + v^2(t - t_0)^2}$$

Impact approximation (III) - Strong collisions

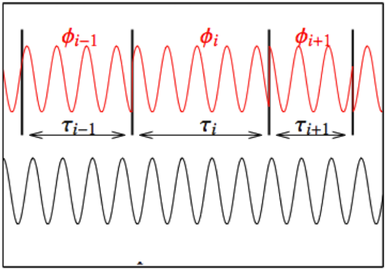

The collisions interrupt the emission of radiation.

The duration of the wave trains follows:

$$W(t) = \frac{1}{\tau} e^{-t\tau} \tag{40}$$

thus

$$C(t) = e^{(i\omega_0 - \frac{1}{\tau})t} \tag{41}$$

and

$$L_{SC}(\omega) = \frac{1}{\pi} \frac{\gamma}{(\omega - \omega_0)^2 + \gamma^2} \tag{42}$$

with $\gamma = 1/\tau$.

Impact approximation (III) - Strong collisions

τ the typical time between collisions so γ is the collision frequency. It is given by:

$$\gamma = \frac{1}{\tau} = N\sigma\langle v\rangle \tag{43}$$

where N is the perturber density, $\langle v\rangle$ is thermal velocity and the collisional cross section.

Following Weisskopf theory,

$$\sigma = \pi\rho_W^2, \tag{44}$$

With $\rho_W = \frac{\hbar n^2}{m_e}\langle v\rangle$ is the Weisskopf radius which determines an effective cross section corresponding to collisions yielding coherence loss of the atomic wavefunction.

Impact approximation (III) - Weak collisions

- collision duration is much shorter than the time of interest.
- $\langle U_I(t)\rangle_{electrons} \equiv \langle_{t=0} \;\; \rightarrow \;\; \rangle_t$: each particle particle independently collides during one Δt,
- $$\langle_{t=0} \;\; \rightarrow \;\; \rangle_t \;=\; \langle_{t=0} \;\; \rightarrow \;\; \rangle_{\Delta t} \cdot \langle_{\Delta t} \;\; \rightarrow \;\; \rangle_{2\Delta t} \cdots \langle_{\Delta t-1} \;\; \rightarrow \;\; \rangle_t \;=\; (\langle_{t=0} \;\; \rightarrow \;\; \rangle_{\Delta t})^N$$
  with $t = N\Delta t$.
- since $\Delta t \ll t$, $N \rightarrow \infty$, then $\langle_{t=0} \;\; \rightarrow \;\; \rangle_{\Delta t} \sim 1 - \phi\Delta t = 1 - \frac{\phi t}{N}$
  and $\langle_{t=0} \rightarrow \rangle_t = (1 - \frac{\phi t}{N})^N = e^{-i\phi t}$
- The autocorrelation function of the dipole is then given by: $C(t) = e^{-\phi t}$.

Impact approximation (IV) - Weak collisions

Using the perturbation theory up to the second-order in the radiator-electron interaction, the Maxwell-averaged operator is given by:

$$\Phi(\Delta\omega) = -\frac{4\pi}{3} N_e \sqrt{\frac{2m}{\pi k_B T_e}} \left(\frac{\hbar}{m}\right) \vec{d} \cdot \vec{d}^{*} \; G(\Delta\omega)$$

There are many ways to estimate the G-function[18]

- related to charge-density fluctuations in the plasma where the dielectric function may be estimated in the Random-Phase Approximation for a Maxwellian plasma[19]
- Asymptotic limits[20] at $\Delta\omega \to 0$ and $\Delta\omega \to \infty$
- Semi-classical GBK model[21]
- ...

[18] see Griem's books
[19] J.W. Dufty, Phys. Rev. 5, 305 (1969).
[20] Lee, R.W., JQSRT 40, 561 (1988).
[21] H.R. Griem,et al. Phys. Rev. A19, 2421 (1979).

Impact approximation (V) - Discussions of the different models

see recent publication of Iglesias[22] and ref thereine, where are discussed:

- the hydrogen Balmer series
- Mg He-like lines profiles, used to characterize plasmas in opacity measurements
- isolated lines

and for the problem in isolated ion lines see Y. Ralchenko, M. Dimitrijevic, S. Sahal-Bréchot, S. Alexiou, RW. Lee.

[22] C.A. Iglesias, HEDP 18, 14 (2016)

Impact approximation (VI) - Influence of interference terms

- The interference terms of the electron-broadening operator couple different transitions together.

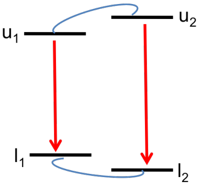

$$\vec{d} \cdot \vec{d} \sim (d^2)_l + (d^2)_u - 2 d_u d_l^*$$

- They correspond to off-diagonal terms in $\phi(\Delta\omega)$ $\rightarrow$ challenging calculations
- When they are non negligible, their effects on the spectral line shape is a reduction of the electronic line width due to the mixing between the involved radiative transitions,[23],[24].

[23] C.A. Iglesias, HEDP 6, 318 (2010)

[24] E. Galtier et al., Phys. Rev. A 87, 033424 (2013)

Impact approx. (VII) - Influence of interference terms

Example on the electron broadening of the Li-like satellites to the Ar He-β line[25]

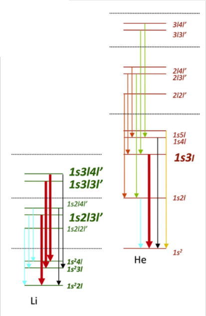

The Li-like satellite line transitions arise from doubly-excited states

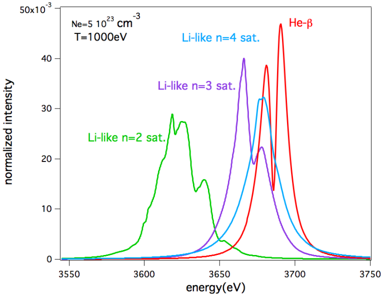

warning the intensity ratios have no meaning

[25] R.C. Mancini et al, HEDP 9, 731 (2013)

Impact approx. (VIII) - Influence of interference terms

Example on the electron broadening of the Li-like satellites to the Ar He-β line[26]

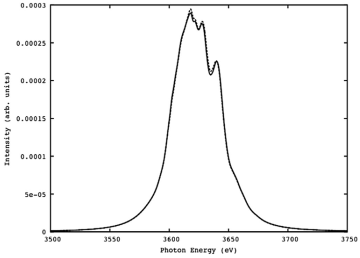

Fig. 2. Spectral line shape of $n = 2$ satellites calculated for $T_e = 1000$ eV and $N_e = 1 \times 10^{24}$ cm^{-3}, without interference term (solid) and with interference term (dash).

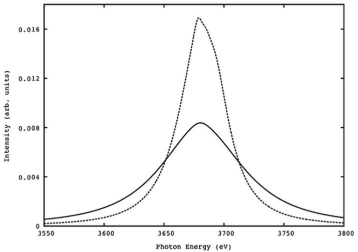

Fig. 4. Spectral line shape of $n = 4$ satellites calculated for $T_e = 1000$ eV and $N_e = 1 \times 10^{24}$ cm^{-3} (top) and $N_e = 2 \times 10^{24}$ cm^{-3} (bottom), without interference term (solid) and with interference term (dash).

Including the interference term in the electron impact broadening of overlapping lines leads to a significant narrowing of the Stark-broadened line shape for transitions involving a high-n spectator electron

[26] R.C. Mancini et al, HEDP 9, 731 (2013)

Validity of the impact approximation

- for hydrogen, ionized helium, etc., the impact approximation is valid for portions of the line shape near the center of the line or within the half-width $\rightarrow$ for $\tau_i \gg \nu_{col}$

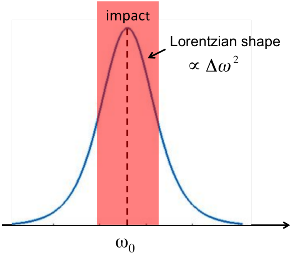

as $\phi \propto n^4 N_e / \sqrt{(}T_e)$ the electron broadening is proportional to N_e.

- For high-n or coupled plasmas, e.g. high densities and low temperatures, it breaks $\rightarrow$ the electrons are more static

- for two and more electron systems, the impact approximation is practically always applicable.

Quasi-static approximation (I)

- The ionic microfields are considered constant during the light emission
- In plasmas, a specific distribution of microfields $W(F)$ produces the F_i
- For a given value of F_i the oscillation frequency of the radiator is shifted by $\omega(F_i)$
- The intensity of the radiation at this frequency is assumed to be proportional the statistical weight of the microfields.

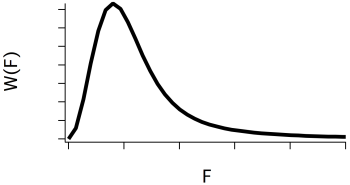

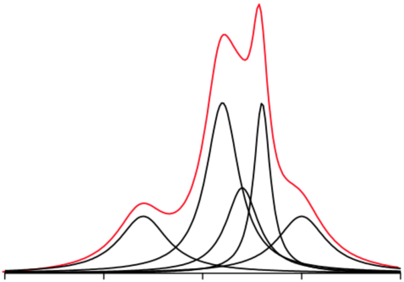

$\rightarrow$ the central problem is to determine the probability distribution of the perturbing microfields

QS approx. (II) - Electric microfield distribution

The microfield distribution $Q(\vec{F})$ is defined as the probability density of finding an electric field $\vec{F}$ equal to $\vec{F}_i$ at particle i equal to at particle i.

$$Q(\vec{F}) = \langle \delta(\vec{F} - \vec{F}_i \rangle, \tag{45}$$

For an isotropic plasma, the distribution $W(F)$ of field strengths is

$$W(F) = 4\pi F^2 Q(\vec{F}) \tag{46}$$

It is convenient to introduce the dimensionless quantity:

$$\beta = F/F_0 \tag{47}$$

with F_0 the normal field strength.
Finally, the distribution $W(\beta)$ is a normalized distribution:

$$\int_0^\infty W(\beta) d\beta = 1 \tag{48}$$

QS approx. (III) - Holtsmark model[27]

- Ensemble of statistically independent pertubers.
- The microfield at the position of the radiators is the superposition of the microfields created by all the perturbers.

$$W(\beta) = \frac{2\beta}{\pi} \int_0^\infty x \cdot sin(\beta x) \cdot e^{-x^{3/2}} dx \qquad (49)$$

- The quasi-static line shape is:

$$L_{QS}(\omega) = \int_0^\infty dF \; W(F) L(\omega, F) \qquad (50)$$

- Considering $\Delta\omega = \omega - \omega(F_i)$,

$$L_{QS}(\Delta\omega) d(\Delta\omega) \propto W(\beta) \frac{d\beta}{d\Delta\omega} d(\Delta\omega) \qquad (51)$$

That leads to line shape with wings $\sim (\Delta\omega)^{-5/2}$.

[27] J. Holtsmark, Ann. d. Phys. 58, 577 (1919)

QS approx. (IV) - Accounting for correlations

In reality, the particles in plasma interact each others → different models have been developed to account for particles correlations in the field distribution function (see the review of A. Demura[28])

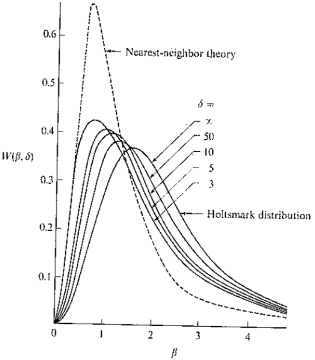

FIGURE 9-1
Probability distribution of field strength at a test point, including shielding effects; δ is the number of charged particles within the Debye sphere. From (**205**), by permission.

- Holtsmark vs Debye shielding model[a]
- $\delta = 4\pi\lambda_D^3 N_e$ is the number of particles contains in the Debye sphere.

[a] G. Ecker, Z.Physik 148, 593 (1957)

[28] A. V. Demura, Int. J. of Spectroscopy 2010, 671073 (2010).

QS approximation (IV) - Accounting for correlations

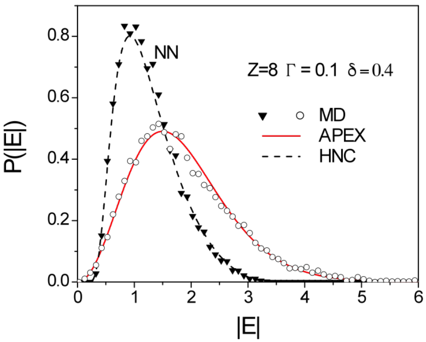

- APEX[a] model (adjustable-parameter exponential)
- computationally fast and suited for weakly as well as strongly coupled plasmas.
- generalized to include separate electron and ion temperatures
- appears to be generally the most accurate in comparison with Monte Carlo (MC)[b] and Molecular Dynamics (MD)[c] results

---

[a] C.A. Iglesias, et al., Phys. Rev. A31, 1698 (1985)
[b] M.S. Murillo et al., Phys. Rev. E55, 6289 (1997).
[c] B. Talin et al., Phys Rev E65, 056406 (2002).

Accounting for correlations - effects on line shapes

H-like Argon Lyman series at $N_e = 10^{24}\ cm^{-3}$ and $T_e = 1keV$.

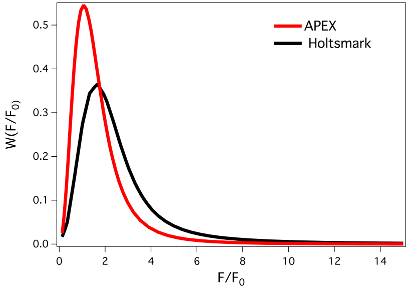

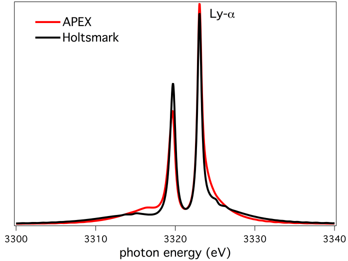

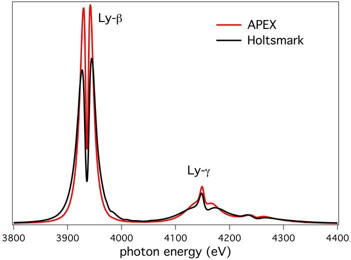

Increasing the electron density (for constant $T_e = 10\ eV$)

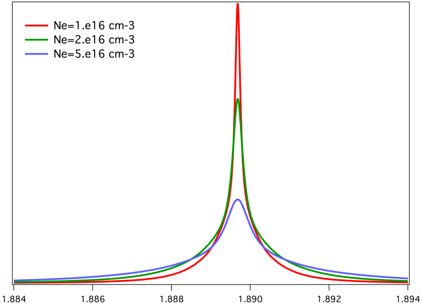

H$-\alpha$ lines

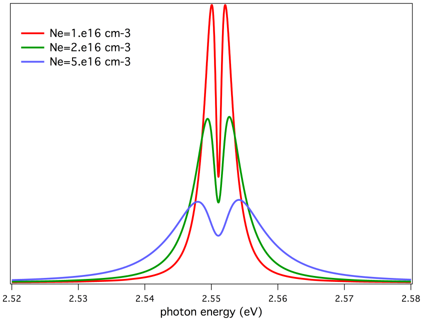

H$-\beta$ lines

Why the H$-\alpha$ line present a central component while the H$-\beta$ lines present a dip at the center of the line?

Effect of the pertubers - ion dynamics (I)

The quasi-static theory works quite well for hydrogen lines but ion dynamics is important[29],[30].

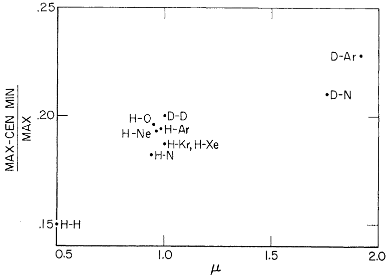

FIG. 1. Relative dip versus reduced mass of the atom-radiator-ion-perturber system. All measurements were made at roughly the same electron density of $(7 \pm 1) \times 10^{16}$ cm^{-3}, which is also roughly at the same arc current.

Relative dips versus reduced mass

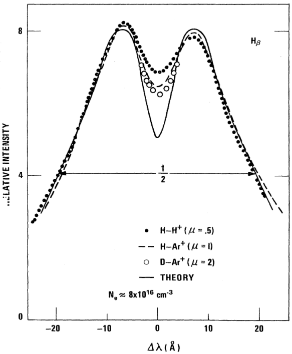

FIG. 6. Central part of the H_β profile at three different values of the reduced mass for $N_e \approx 8 \times 10^{16}$ cm^{-3}. Since

Central part of the $H-\beta$ lines

[29]D.E. Kelleher, Phys. Rev. Lett. 24, 1431 (1973)

[30]W.L. Wiese et al., Phys. Rev. A 11, 1854 (1975).

Ion dynamics (II)

Theoretical and experimental time-resolved spectroscopic investigation of indirectly driven microsphere implosions[31] where several fill gases with a trace amount of argon were used.
$\rightarrow$ analysis of the line profile of Ar XVII $1s^2 - 1s3p\ ^1P$ (Ar He$-\beta$ lines).

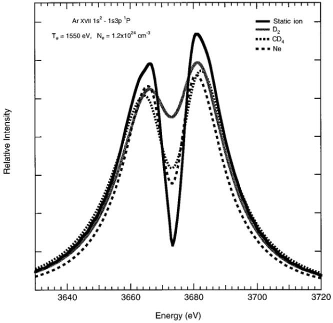

Relative dips versus reduced mass

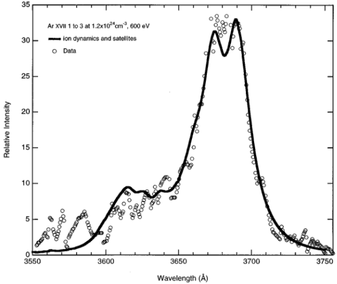

Ar He$-\beta$ lines with Li-like satellites accounting for the ion dynamics.

[31] N.C. Woolsey et al., Phys. Rev.E 53, 6396 (1996).

Methods for solving the ion dynamics

Taking into account the stochastic electric fields at emitters has been an issue since the '60s (see Griem's book and Alexiou[32]).

The main difficulty in introducing the ion dynamics in the Stark line shape calculations is to develop a model that provides a sufficiently accurate solution of the evolution equation assuming an idealized stochastic process that conserves the statistical properties of the "real" interaction between the microfields and the radiating atom.

Different stochastic models

- Numerical Simulations
- Method of Model Microfield (MMM) [33]
- Boercker, Iglesias, Dufty's model (BID)[34]
- Frequency Fluctuation Model (FFM)[35,36]

[32] S. Alexiou, HEDP **5**, 225 (2009)
[33] U. Frisch and A. Brissaud, JQSRT **11**, 1753(1971)
[34] D. Boercker, C. Iglesias and J. Dufty, PRA **36**, 2254 (1987)
[35] B. Talin et al., PRA **51**, 1918 (1995)
[36] A. Calisti et al., PRE **81**, 016406 (2010)

Method of Model Microfield[37] (MMM)

Describing the interaction of the plasma and the atomic dipole by an effective stochastic field that reproduces the statistical properties of the "real" microfield:

- static properties: $W(\vec{F})$
- dynamics properties: $< \vec{F}(t) \cdot \vec{F}(0) >$

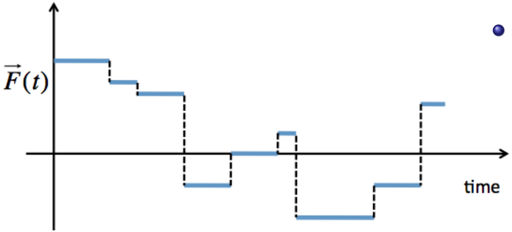

- the microfield is supposed to be constant in a given time interval,
- the jumping frequency $\nu(\vec{F})$ is a free parameter that must be chosen properly

[37] U. Frisch and A. Brissaud, JQSRT **11**, 1753(1971)

BID[38]

Its formulation is based on the kinetic model and is extended to charged emitters.

- the stochastic line-shape is written as:

$$I(\omega) = -\frac{1}{\pi} Im Tr \left[\vec{d}^* \frac{\int d\vec{F} W(\vec{F}) G(\omega, \vec{F})}{1 + i\nu(\omega) \int d\vec{F} W(\vec{F}) G(\omega, \vec{F})} \vec{d} \rho_0 \right], \qquad (52)$$

- in which the resolvent is given by:

$$G(\omega, \vec{F}) = \left(\omega - L_0 + \frac{1}{\hbar} \vec{d} \cdot \vec{F} - i\nu(\omega) \right)^{-1} \qquad (53)$$

- the jumping frequency is chosen as: $\nu(\omega) = \frac{\nu_0}{1 + i\omega\tau}$, where ν_0 and τ are defined by the low- and -high-frequency limits of the momentum autocorrelation function $\overline{C}_{pp}(\omega)$.

[38] D. Boercker, C. Iglesias and J. Dufty, PRA **36**, 2254 (1987)

Frequency Fluctuation Model (FFM)[39,40]

The FFM is based on the premise that a quantum system perturbed by an electric microfield behaves like a set of field dressed two-level transitions, the Stark dressed transitions (SDT) and that the microfield fluctuations produce frequency fluctuations.

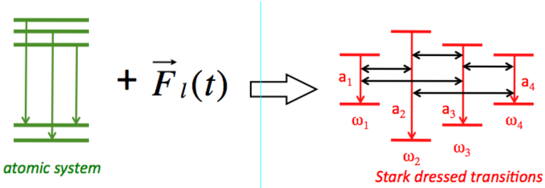

If the microfield is time varying, the transitions are subject to a collision-type mixing process induced by the field fluctuations.

[39] B. Talin et al., PRA **51**, 1918 (1995)
[40] A. Calisti et al., PRE **81**, 016406 (2010)

Frequency Fluctuation Model (FFM)[41,42]

The stochastic line-shape is written as:

$$I(\omega) = \frac{r^2}{\pi} Re \frac{\sum_k \frac{(a_k + ic_k)/r^2}{\nu + \gamma_k + i(\omega - \omega_k)}}{1 - \nu \sum_k \frac{(a_k + ic_k)/r^2}{\nu + \gamma_k + i(\omega - \omega_k)}} \tag{54}$$

with $r^2 = \sum_k a_k$.

$$\xrightarrow[\textit{contineous}]{} I(\omega) = \frac{\vec{d}^2}{\pi} Re \frac{\int \frac{d\omega' W(\omega')}{\nu + i(\omega - \omega')}}{1 - \nu \int \frac{d\omega' W(\omega')}{\nu + i(\omega - \omega')}} \tag{55}$$

[41] B. Talin et al., PRA **51**, 1918 (1995)
[42] A. Calisti et al., PRE **81**, 016406 (2010)

Solving the ion dynamics (I)

- **MMM**
  - **tabulated Stark-broadening profiles for H lines**: C. Stehlé and R. Hutcheon, Astron. Astrophys. Suppl. Series 140, 93 (1999). B.W. Acon et al., Spectrochimica Acta Part B: Atomic Spectroscopy 56, 527 (2001).
  - **QuantST.MMM** S. Lorenzen, Plasmas. Contrib. Plasma Phys., 53, 368 (2013).
- **BID**
  - **MERL** R. C. Mancini et al., Plasmas. Comput. Phys. Commun, 63, 314322 (1991).
  - **MELS** C.A. Iglesias, High Energy Density Phys. 6, 399 (2010).
- **FFM**
  - **PPP**: A. Calisti, Phys. Rev. A 42, 5433 (1990).
  - **PPPB**: S. Ferri, Phys. Rev. E 84, 026407 (2011).
  - **QC-FFM**: E. Stambulchik et al., AIP Conf Proc 1438, 203 (2012).
  - **FST**: S. Alexiou, HEDP 9, 375, (2013).
  - **QuantST.FFM** S. Lorenzen, Plasmas. Contrib. Plasma Phys., 53, 368 (2013).
  - **ZEST**: F. Gilleron et al., Atoms 6, 11 (2018).
  - **ALICE**: E.G. Hill et al., HEDP 26, 56 (2018).

Quasi-Contiguous FFM model[43]

For Rydberg transitions, the intensity of Stark components on average can be substituted with a rectangular shape.

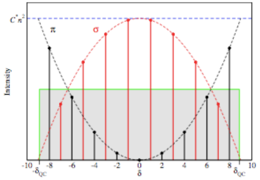

inclusion of the FFM and introduction of an effective ν in order to give the correct impact limit:

$$\nu \rightarrow \begin{cases} \nu & \text{if } |\Delta\omega|/\nu \gg 1 \\ \propto \nu^2 & \text{if } |\Delta\omega|/\nu \ll 1 \end{cases} \qquad (56)$$

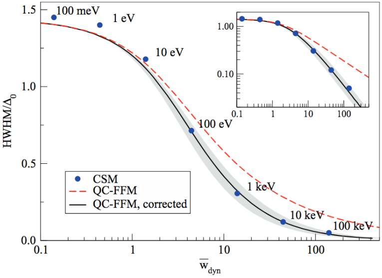

FIG. 5. (Color online) HWHM of the Stark broadening of H Lyδ under the same conditions as in Fig. 4. QC-FFM: line shapes calculated by Eq. (29); QC-FFM, corrected: line shapes calculated

[43] E. Stambulchik et al., Phys. Rev. E87, 053108 (2013)

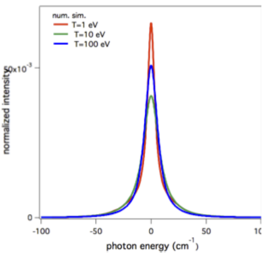

$N_e = 10^{17} cm^{-3}$

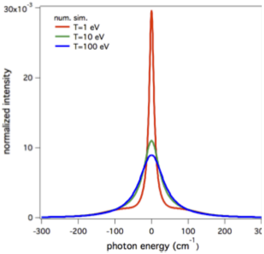

$N_e = 10^{18} cm^{-3}$

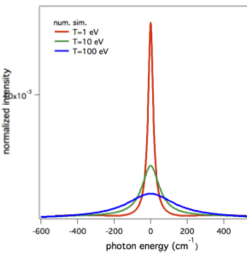

$N_e = 10^{19} cm^{-3}$

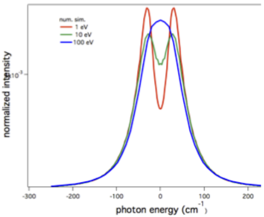

$N_e = 10^{17} cm^{-3}$

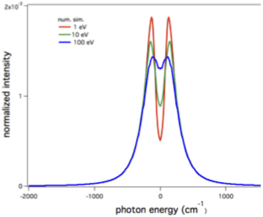

$N_e = 10^{18} cm^{-3}$

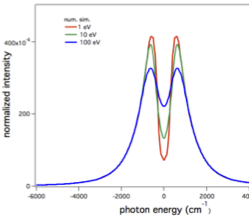

$N_e = 10^{19} cm^{-3}$

[44] S. Ferri et al., Atoms **2**, 299 (2014)

Overall comparison [45]

from the 2nd SLSP code comparison workshop, Vienna, Austria, August 5-9, 2013.

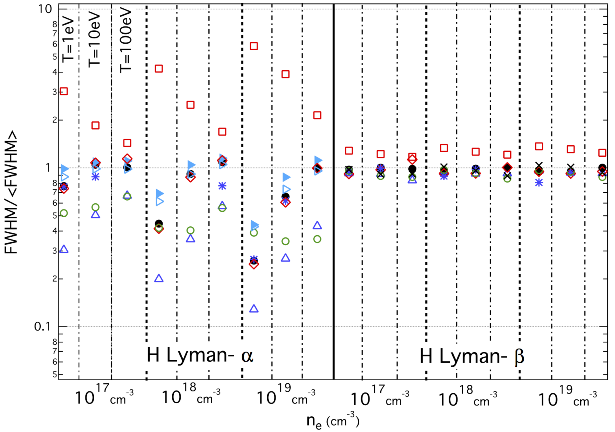

[45] S. Ferri et al., Atoms **2**, 299 (2014)

Influence of microfield directionality

He II Lyman-α line in OCP protons[46,47]

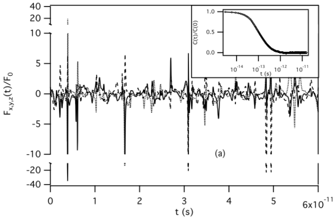

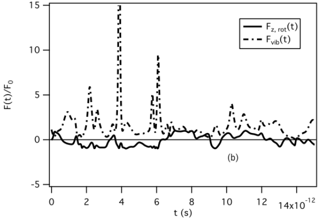

$n_e = 10^{18}\ cm^{-3}$ and $T = 1eV$

vibrational microfield: $\vec{F}_{vib}(t) = \vec{n}_z |\vec{F}(t)|$

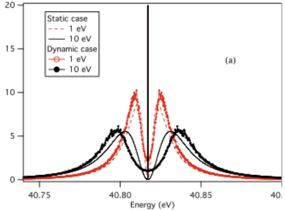

rotational microfield: $\vec{F}_{rot}(t) = F_0 \dfrac{\vec{F}(t)}{|\vec{F}(t)|}$

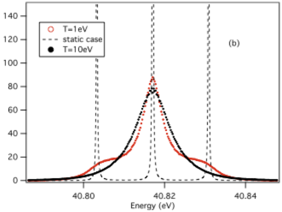

---

[46] A. Calisti et al., Atoms **2**, 259 (2014)
[47] A. Demura et al., Atoms **2**, 334 (2014)

BID / FFM comparisons

Good agreement between the different techniques[48].

It has to be point out that if the same ν is used BID and FFM leads to the same results.

Argon XVII He-β line

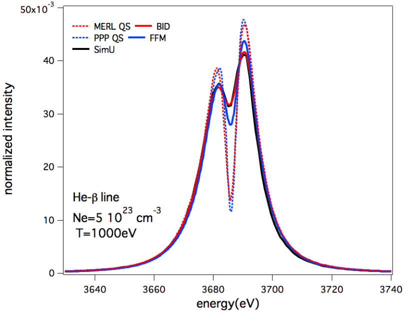

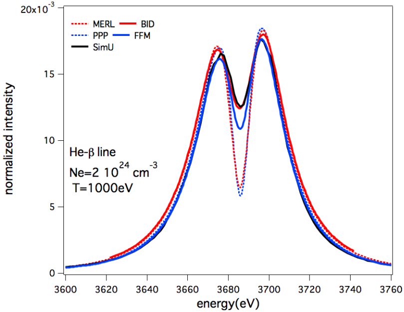

Relative Deep:

$$RD = \frac{I_{dyn}(\omega-\omega_0)-I_{stat}(\omega-\omega_0)}{I_{dyn}(\omega-\omega_0)}$$

models	BID	FFM
$N_e = 5 \cdot 10^{23}\ cm^{-3}$	58%	57%
$N_e = 1 \cdot 10^{24}\ cm^{-3}$	50%	51%
$N_e = 2 \cdot 10^{24}\ cm^{-3}$	47%	48%

[48] S. Ferri et al, Atoms 2, 299 (2014)

Overview

To summarize

Line shapes are (still) fun !!

To summarize... Where to go if I need data?

- **NIST**: Atomic Spectral Line Broadening Blibliographic Database
  https://physics.nist.gov/cgi-bin/ASBib1/LineBroadBib.cgi

- **Stark-B Database**
  http://stark-b.obspm.fr/

- **Stark broadening biblio**: University of Kentucky, KY
  http://www.pa.uky.edu/~verner/stark.html

- **or ask the line broadeners**
  - International Conference on Spectral Line Shapes (ICSLS)
    https://www.icsls2018.com/
  - Spectral Line Shapes in Plasmas code comparison workshop (SLSP)
    http://plasma-gate.weizmann.ac.il/slsp/
  - International Conference on Atomic Processes in Plasmas (APIP)
    https://pml.nist.gov/apip2019/
  - International Workshop on Radiative Properties of Hot Dense Matter (RPHDM)
    https://indico.desy.de/indico/event/18869/

5th SLSP meeting will be held in Vrdnik, Serbia, May 27 - 31, 2019

http://plasma-gate.weizmann.ac.il/slsp/

Except for limiting cases, line-shape calculations imply a usage of computer codes of varying complexity and requirements of computational resources. However, studies comparing different computational and analytical methods are almost nonexistent. This workshop purports to fill this gap. By detailed comparison of results for a selected set of case problems, it becomes possible to pinpoint sources of disagreements, infer limits of applicability, and assess accuracy.

Organizing committee:

- A. Calisti (CNRS, France)
- H.-K. Chung (GIST, Republic of Korea)
- M. Á. González (U. of Valladolid, Spain)
- E. Stambulchik (WIS, Israel)

Books and reviews

- Griem, H.R., Plasma Spectroscopy, McGraw-Hill, New York, (1964).
- Griem, H.R., Spectral Line Broadening by Plasmas, Academic, New York, (1974).
- Griem, H.R., Principles of Plasma Spectroscopy, Cambridge University Press, Cambridge, (1997).
- Mihalas, D., *Stellar Atmospheres*, The University Press Chivago (1978).
- N. Konjević, *Plasma broadening and shifting of non-hydrogenic spectral lines: present status and applications*, Physics reports. (316) 6., 339 (1999)
- H.-J. Kunze, *Introduction to Plasma Spectroscopy*, Springer-Verlag Berlin Heidelberg (2009).
- Alexiou, S., *Overview of plasma line broadening*, High Energy Density Physics 5, 225 (2009)
- E. Stambulchik and Y. Maron, *Plasma line broadening and computer simulations: A mini-review*, High Energy Density Phys. 6, 914 (2010).

This lecture has been prepared with the help of various lectures given by others.

In particular:

- *Line shapes and broadening*, Yuri Ralchenko (Maryland, USA).
- *An overview of spectral line broadening*, Dick Lee, University of Berkeley (California, USA).
- *HED plasma spectroscopy*, Roberto Mancini, University of Reno (Nevada, USA).
- *Spectral lineshape modeling, state of the art*, Annette Calisti (Marseille, France).

Many thanks to them ☺